Journal of Physiology (1989), **413**, *pp.* 563–593
With 11 *text-figures*
Printed in Great Britain

CONTRIBUTION OF HUMAN SHORT-WAVE CONES TO LUMINANCE AND MOTION DETECTION

BY J. LEE AND C. F. STROMEYER III*

From the Division of Applied Sciences, Harvard University, Cambridge, MA 02138, USA

(*Received 20 April 1988*)

SUMMARY

1. Human short-wave S cone signals are important for colour vision and here we examine whether the S cone signals also contribute to motion and luminance.

2. Detection was measured with moving patterns that selectively stimulated S cones – violet sine-wave gratings of 1 cycle deg^{-1} on an intense yellowish field. For rates up to 12 Hz, detection was governed by non-directional mechanisms, possibly of a chromatic nature, as shown by three findings: moving gratings had to be suprathreshold for their direction to be identified; the threshold ratio of counterphase flickering *versus* moving gratings was low; and direction-selective adaptation was essentially absent.

3. Evidence for less sensitive, directional mechanisms includes the following: at high velocity, the direction of movement of the violet gratings can be identified just slightly above the detection threshold; directional adaptation was strong with a suprathreshold test pattern; velocity was seen veridically for clearly suprathreshold patterns; and a counterphase flickering test, added in spatial–temporal quadrature phase to a similar suprathreshold mask, had identical detection and direction–identification thresholds.

4. Interactions of long-wave L cone and S cone signals in direction-selective mechanisms were measured with an orange counterphase grating and a violet counterphase test, both flickering at the same rate and presented in spatial quadrature phase on the yellowish adapting field. Direction identification thresholds, measured as a function of the temporal phase of two gratings, demonstrated both that the S cone signal lags considerably behind the L cone signal (an effect that strongly varies with S cone light adaptation), and more strikingly, the S cone signal summates with a negative sign and thus is effectively inverted in direction-selective mechanisms.

5. Quantitatively similar temporal phase functions were obtained with uniform violet and orange flicker when a luminance discrimination criterion was used: thus the S cone signal summates negatively with the L cone signal for both discrimination of luminance flicker and the direction of motion.

6. The temporal phase functions accurately predicted threshold summation for

* To whom correspondence should be sent.

identifying the direction of motion of a pair of violet and orange gratings moving with the same velocity but with different spatial phase offsets. Once the relative temporal phase lag of the S cones was compensated for, there was linear threshold summation for the violet and orange patterns when presented in effective (physiological) spatial antiphase, and clear cancellation when presented in phase. This and related experiments show a linear summation of S, M and L cone signals for direction detection, with the S cones having a negative sign. The luminance contrast sensitivity is very high for the spectrally long-wave member of the pair of gratings (300–500 at 8 Hz), suggesting that the patterns are detected with high-contrast-sensitivity mechanisms such as the magnocellular pathway, which is known to have S cone input. The present measurements show that the contribution of the S cones to motion detection is only 1/30–1/50 that of the M and L cones, expressed in units of the cone contrasts of the component gratings. Thus the most sensitive mechanisms detecting rapid motion have a weak S cone input.

7. A sudden dimming of the yellowish adapting field strongly reduces the S cone, but not the M cone, input into the directional mechanisms. This 'transient tritanopia' suggests that S cone signals proceed through a spectrally antagonistic site before summation in directional mechanisms.

INTRODUCTION

A widely held view, based on human psychophysics, is that signals originating in the short-wave (S) cones have access only to spectrally antagonistic pathways that serve colour vision (Mollon & Krauskopf, 1973; Pugh & Mollon, 1979; Friedman, Yim & Pugh, 1984). This hypothesis is strongly supported (Pugh & Mollon, 1979) by various anomalies of light adaptation: changing the intensity of a bluish or yellow adapting field can produce unexpectedly large changes in the threshold of a violet flash detected via the S cones. These results have been explained by postulating that the S cone signals proceed through a spectrally antagonistic site that is strongly polarized by sudden large changes in the ratio of the adaptational signals from the short-wave cones relative to the middle- (M) and long-wave (L) cones (Pugh & Mollon, 1979).

The present investigation examines the degree to which the S cone signals contribute to luminance and motion. Eisner & MacLeod (1980), using heterochromatic flicker photometry, and Cavanagh, MacLeod & Anstis (1987), using nulling of apparent motion, were unable to identify an S cone contribution. Stockman, MacLeod & DePriest (1987), however, observed that rapid violet flicker on an intense orange adaptation field could null red flicker, indicating an interaction of S and L cones in luminance flicker discrimination. They further observed that the S cone signal summates with a negative or inverted sign for luminance judgements.

We conducted three series of experiments. The first used several well-known protocols for measuring directional motion mechanisms in human vision, to determine whether directional selectivity can also be demonstrated for stimuli that essentially stimulate only the S cones, namely for violet test patterns on an intense yellowish adapting field. The second series employed pairs of different coloured stimuli to examine interactions of signals from the different spectral classes of cones.

The relative phase response of S and L cone signals was measured for both motion and luminance flicker discrimination. The S cone signals lag in phase and in addition summate negatively with the L cone signals, and the phase functions are essentially similar for both tasks. Threshold summation for pairs of moving gratings of different colours indicates that the most sensitive mechanisms for detecting rapid motion have a weak S cone input of negative sign. The third series of measurements show that prior to this summation in motion detectors, the S cone signals initially proceed through a spectrally antagonistic site that can be strongly polarized by sudden dimming of the yellow adapting field.

METHODS

Stimuli and spectral calibration

Vertical coloured sine-wave gratings were superposed on an intense adapting field of a different colour. The S cones were isolated with violet test patterns on an intense yellow–green or orange adapting field.

The apparatus is represented in Fig. 1. The adapting fields, seen in Maxwellian view, were derived from 50 W halogen lamps, S. The light passed through narrow-band interference filters, IF. The Maxwellian lens, ML, focused the beams on an artificial pupil, AP (3 mm), and achromatizing lens, AL, that corrects for the eye's longitudinal chromatic aberration. Two final relay lenses, L, formed a 3 mm image of the artificial pupil in the observer's pupil. Field stops, FS, defined the border of the stimuli: the circular adapting field subtended 4·2 deg, while the grating subtended 4 deg diameter. There was a black fixation point in the centre of the field. The observer was steadied with a dental impression on a rigid translator. His eye was positioned in the x–y–z dimensions relative to the final lens so that a pair of superposed different-coloured adapting fields (e.g. yellow–green and violet) appeared coincident, and hence chromatic aberration was corrected over the 4·2 deg field.

The gratings, generated with an Innisfree Image Synthesizer, function generators and a DEC PDP 11/34a computer (with 12-bit DACs), were displayed on Tektronix 608 CRT monitors. Three CRTs with different phosphors were used singly or in pairs. They were optically combined with a dichroic mirror, DM, and thence joined with the adapting fields with a beam-splitter cube, BSC_1, which attenuated the light from the CRTs by only 20%. The CRT phosphors decayed to 1/10 in $< 1{\cdot}2$ ms and the frame rate was 106·2 Hz.

The violet CRT (P11 phosphor) was filtered with a 460 nm short-pass interference filter, F; the measured spectral centroid of the light at the eye (see below) was 441 nm based on quantal flux (423–459 nm half-bandwidth). The intensity control knob of the violet CRT, which affects linearity, was set so that the DC shift at contrasts as high as 60% was $< 0{\cdot}5$%; thus spatial patterns could not be detected with S cones by a uniform violet colour shift. The green CRT (P31 phosphor) was filtered with a Wratten 55 filter (the light had a spectral centroid of 538 nm; 512–562 nm half-bandwidth). The orange CRT (P22 custom phosphor) was filtered with a Wratten 21 filter when used with the yellow–green adapting field and a Wratten 26 filter when used with the orange field. The orange light had a spectrum of narrow bands, with most energy at 627 nm and much less at 618 and 707 nm (with the Wratten 21 filter, there was also a weak band at 596 nm). The yellow–green and orange adapting fields were of 559 and 619 nm respectively (9 nm half-bandwidth).

A weak uniform violet field of 442 nm (9 nm half-bandwidth) could be added to demonstrate isolation of the S cones; the field and violet grating, when equated in quantal flux, produced virtually equivalent quantal catches in the S cones. The violet field dilutes the S cone contrast, but does not significantly affect the M and L cones, since they are much more light-adapted by the intense long-wave adapting field. Thus, if the added violet field raises the threshold of the violet pattern, the pattern is probably detected with S cones. This method was developed by Stiles (1953) to separate the short-wave and middle-wave π mechanisms.

Radiance calibrations were made each session with a calibrated radiometer placed at the eyepiece. Spectral calibrations of all stimuli were also made at the eyepiece over the range 350–750 nm, using a monochromator with 2 nm half-bandwidth. The resultant spectral radiance curves

(corrected for the monochromator transmission and radiometer spectral response) were weighted by the quantal-basis version of the S, M and L cone fundamentals of Smith & Pokorny (1975) to calculate the contrast of the gratings for each cone class. For example, S cone contrast is defined as $\Delta S/S$, where ΔS is one-half of the amplitude of the S cone quantal catches owing to the spatially varying component of the grating, and S is the mean S cone quantal catch owing to *all* the light components. (The factor of one-half normalizes maximal contrast to 1·0.) In the calculation of cone contrast, we ignored observer variation in macular pigment density and variation in the action

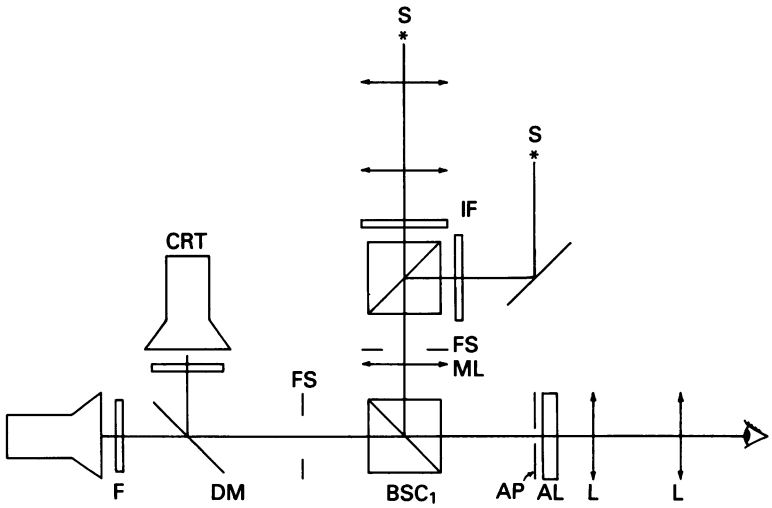

Fig. 1. Optical apparatus for producing pairs of coloured gratings superposed on intense chromatic adapting fields seen in Maxwellian view. One CRT was typically violet and the other orange. For abbreviations see Methods.

spectrum of the M and L cones due to bleaching by the intense yellow-green adapting fields of 30000–44000 td. Bleaching would reduce the contrast of the violet and orange gratings for the M and L cones by 15–20% (Hollins & Alpern, 1973), and this small factor does not affect our conclusions.

General methods

The luminance profile of a vertical, moving sine-wave grating is represented by

$$L(x,t) = L_0[1 + m\cos(2\pi fx \pm 2\pi\omega t)],$$

where L_0 is mean luminance, m is grating contrast, f is spatial frequency (cycles deg^{-1}), x is the horizontal position of the grating (deg), ω is the rate of horizontal movement (Hz) and t is time (s). Two gratings of the same spatial frequency, moving at the same rate in opposite directions, are represented by

$$L(x,t) = L_0[1 + m_{\text{left}}\cos(2\pi fx + 2\pi\omega t) + m_{\text{right}}\cos(2\pi fx - 2\pi\omega t)].$$

If the contrast of each is m', a standing wave is formed that sinusoidally reverses contrast, represented by

$$L(x,t) = L_0[1 + 2m'\cos(2\pi fx)\cos(2\pi\omega t)].$$

The peak contrast of this counterphase grating is twice the contrast of either of its right- or left-moving components. If the moving components are detected independently by directionally selective mechanisms, then the threshold of the counterphase grating should be approximately twice the threshold of either of the moving components (Levinson & Sekuler, 1975). This relationship will be tested with gratings that stimulate S cones.

Interactions between signals from different classes of cones in generating motion were measured

with a 'quadrature phase' protocol (Stromeyer, Kronauer, Madsen & Klein, 1984). A fixed-contrast counterphase grating was used as a 'mask', and a similar counterphase test grating of variable contrast was added in spatial–temporal quadrature phase (shifted in phase by $\pi/2$ rad in space and time relative to the mask) so as to decrease the right component of the mask and increase the left component by the same amount, or conversely. The latter combination can be represented as

$$L(x,t) = L_0[1 + (m_{\text{left}} - \Delta)\cos(2\pi fx + 2\pi\omega t) + (m_{\text{right}} + \Delta)\cos(2\pi fx - 2\pi\omega t)].$$

The test decreases the left component ($-\Delta$) and increases the right component ($+\Delta$) by an equivalent amount. The expression for this test-plus-mask can be rewritten as

$$L(x,t) = L_0[1 + 2m'\cos(2\pi fx)\cos(2\pi\omega t) + 2\Delta\sin(2\pi fx)\sin(2\pi\omega t)],$$

in which $m' = m_{\text{left}} = m_{\text{right}}$. The cosine terms represent the counterphase mask, and the sine terms represent the quadrature counterphase test. An important point is that the motion produced by the test can be reversed by simply shifting its temporal phase by 180 deg. Interactions of signals from different classes of cones in generating motion were measured by presenting the counterphase mask and test in different colours, as explained later.

Thresholds were measured with a two-alternative forced-choice (2AFC) staircase: each trial had two temporal intervals of 1356 ms, signalled by tones and separated by 100 ms. One interval selected at random contained the test pattern. The patterns were ramped on for 339 ms with a raised cosine function, held constant for 678 nm and then ramped off with the raised cosine. (The envelope was expanded twofold for 1 Hz stimuli.) The test contrast dropped 0·10 log unit when the observer was right twice in a row, and rose an equivalent step when he was wrong once, thus estimating 71% correct detection (Wetherill, 1963). Tones provided response feedback. Two or more independent staircases were interleaved in a run. Each threshold estimate was defined as the geometric mean of the final six of eight reversals of four to twelve separate staircases; error bars represent $\pm 1{\cdot}0$ S.E.M. of the reversals. We measured thresholds for detecting a pattern or thresholds for identifying whether the pattern moved leftwards or rightwards. The observer stared at the central fixation point during all presentations. The observers had normal colour vision.

RESULTS

I. *Tests for whether motion is signalled by the S cones*

We first tested whether the S cones contribute to motion, using several well-known protocols. Unless stated otherwise, dim vertical violet gratings (441 nm; 8·76 log quanta $\text{deg}^{-2}\,\text{s}^{-1}$; 21 td) were presented on an intense yellow–green adapting field (559 nm; 10·74 log quanta $\text{deg}^{-2}\,\text{s}^{-1}$; 43900 td). The adapting field strongly reduces sensitivity of the M and L cones while having little effect on the S cones, and thus the violet patterns are probably detected with the S cones, as was confirmed.

Thresholds for counterphase versus moving gratings and thresholds for identifying the direction of the moving gratings

Since a counterphase grating can be analytically decomposed into two equivalent oppositely moving gratings, the contrast threshold ratio of counterphase *versus* moving gratings may approach 2·0 if the moving components are detected independently. For achromatic gratings, this ratio approaches 1·8–2·0 for rapidly moving patterns (Levinson & Sekuler, 1975; Watson, Thompson, Murphy & Nachmias, 1980; Stromeyer *et al.* 1984) but falls to a much lower value for slowly moving patterns detected by non-directional mechanisms (Watson *et al.* 1980). When the ratio is high, the direction of movement can be identified at the detection threshold; when the ratio is low, the moving grating must be raised above the detection threshold to identify its direction (Watson *et al.* 1980).

Table 1 shows contrast thresholds (expressed as S cone contrast) of violet gratings of 1 cycle deg^{-1} at temporal frequencies spanning 2 octaves (2·95–11·8 Hz). The top and bottom halves of the table are for observers C.F.S. and J.L. respectively. Thresholds were measured for detection of the counterphase (C) and moving gratings (M) and for identifying (I) the direction of the moving gratings. The threshold ratio for counterphase and moving gratings (C/M ratio) varies little with temporal frequency and has a low value of 1·3–1·5, implying that the patterns are detected by non-directional mechanisms.

TABLE 1. Thresholds for violet gratings of 1 cycle deg^{-1}: detection of counterphase (C) and moving gratings (M) and identification of direction of motion (I)

Frequency (Hz)	Task	S cone contrast (%)	C/M ratio	I/M ratio
		Observer C.F.S.		
	C	2·99 ± 0·13		
2·95	M	2·26 ± 0·09	1·32	3.48
	I	7·87 ± 0·46		
	C	7·04 ± 0·28		
5·9	M	4·64 ± 0·19	1·52	1·96
	I	9·08 ± 0·32		
	C	25·5 ± 1·06		
11·8	M	18·0 ± 0·65	1·42	1·19
	I	21·5 ± 0·86		
		Observer J.L.		
	C	3·57 ± 0·21		
2·95	M	2·72 ± 0·13	1·31	2·09
	I	5·69 ± 0·36		
	C	7·46 ± 0·40		
5·9	M	5·45 ± 0·30	1·37	2·11
	I	11·5 ± 0·52		
	C	27·2 ± 1·28		
11·8	M	21·4 ± 0·91	1.27	1.35
	I	28·8 ± 1·06		

At the lower temporal frequencies of 2·95 and 5·9 Hz, the counterphase and moving gratings near the detection threshold appeared to have yellow and whitish stripes without flicker or motion. The threshold ratio for identification and detection of the moving gratings (I/M ratio) shows that the gratings had to be raised 2–3 times above detection threshold to identify direction. The stimulus field contained dust and the fixation point, but surprisingly, movement of just-suprathreshold stripes past these stationary marks did not allow the direction to be seen.

At the higher temporal frequency of 11·8 Hz, the direction of motion was identified at only 19–35% above detection threshold. This low I/M ratio might possibly have been caused by spatial displacement clues rather than by true motion signals, although C.F.S. remarked that he generally saw motion slightly above the detection threshold. As a control, we repeated the 11·8 Hz experiment with a low spatial frequency of 0·12 cycles deg^{-1} to help eliminate apparent spatial structure in the

grating. For C.F.S., the I/M ratio was 1·24, and the grating appeared as formless left or right racing motion at the identification threshold.

The moving gratings were detected with S cones as shown by two considerations. First, the contrast of the gratings is presumably too low for the gratings to be detected by the M and L cones: a violet grating that produces S cone contrast of 20% in Table 1, produces M and L cone contrast of only 0·018 and 0·010%. Second, adding a weak uniform field of violet light (442 nm, 9·03 log quanta deg^{-2} s^{-1}) caused the threshold of the 5·9 and 11·8 Hz moving grating to rise 2·8 and 2·3 times respectively (observer C.F.S.). The added field dilutes the S cone contrast 2·6 times but has virtually no effect on the M and L cone contrast (an effect of $\ll 1\%$).

In summary, the low detection ratios for counterphase and moving gratings show that the patterns are presumably not detected by direction-selective mechanisms. The direction of motion cannot be correctly identified near threshold even when moving as fast at 6 deg s^{-1} (6 Hz). However, at 12 Hz the direction of motion of the grating is apparent when the grating is just slightly above threshold.

TABLE 2. Direction-selective adaptation for moving violet gratings (1 cycle deg^{-1}, 5·9 deg s^{-1}): S cone contrast (%) thresholds for left and right test movement after left or right adaptation

Test movement	Left adaptation	Right adaptation
	Observer C.F.S.	
Left	13·8 ± 0·95	11·3 ± 0·61
Right	10·2 ± 0·88	13·9 ± 0·96
	Observer J.L.	
Left	11·5 ± 0·86	9·3 ± 0·85
Right	12·0 ± 1·17	15·5 ± 0·92

Direction-selective adaptation

We next attempted to measure direction selectivity with a pattern adaptation protocol in which prolonged viewing of an adapting grating moving in one direction may selectively elevate the detection threshold for a test grating moving in the same direction compared to the opposite direction (Sekuler & Ganz, 1963).

A moving adapting grating of 65% S cone contrast was presented for 6 s between each test trial. The observer initially viewed the adapting pattern for several minutes.

Table 2 shows detection thresholds for rightward and leftward moving test gratings measured with adaptation to either rightward or leftward motion in separate runs. Each threshold was based on six staircases. The patterns were of 1 cycle deg^{-1}, moving at 5·9 deg s^{-1} (5·9 Hz). The unadapted thresholds are $\sim 5\%$ (Table 1), and thus adaptation raises the threshold for both right and left tests by 2–3 times. The direction selectivity of adaptation is very small, although it is statistically significant (*t* test, $P < 0{\cdot}05$) for C.F.S. and for J.L. for rightward adaptation. The experiment was repeated with the patterns raised in spatial frequency to 3 cycles deg^{-1}: for both observers, adaptation again elevated the threshold 2–3 times, but direction selectivity did not reach statistical significance (results now shown).

For the above measurements, direction selectivity was examined with the test pattern at its detection threshold. Adaptation may have reduced the sensitivity of both directional and non-directional mechanisms, and the essential lack of direction selectivity might be explained if the non-directional mechanisms help detect these threshold-level test patterns. Directional adaptation was next examined with a *suprathreshold* test pattern using a method suggested by observations of Levinson & Sekuler (1975). They remarked that adaptation to a moving grating caused a

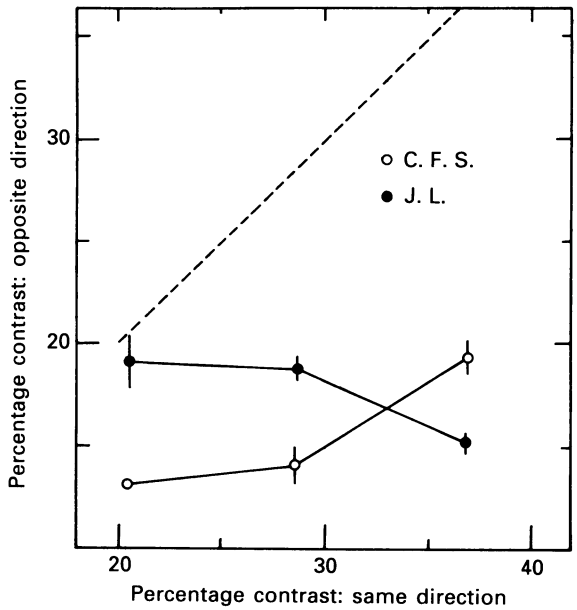

Fig. 2. After-effect of adapting to a violet grating of 1 cycle deg^{-1}, and 65% S cone contrast ($\Delta S/S$), moving in one direction at 5·9 deg s^{-1} on an intense yellow-green adapting field. The suprathreshold test pattern was a pair of oppositely moving violet gratings (1 cycle deg^{-1}, 5·9 deg s^{-1}), one moving in the same direction as the adapting pattern and fixed in contrast (abscissa), and the other moving in the opposite direction and adjusted in contrast (ordinate) to null motion of the combined test pattern. Points below the dashed line demonstrate direction-selective adaptation, because test motion in same direction as the adapting pattern is less effective than test motion in the opposite direction. Contrast is specified as S cone contrast.

counterphase flickering test grating to appear to move with a uniform velocity in the opposite direction. We repeated our adaptation experiment, using a hybrid 'counterphase' test pattern, which was presented in a single test interval immediately following each adapting presentation. The hybrid test consisted of a pair of similar, oppositely moving violet gratings: the component that moved in the same direction as the adapting pattern was held constant at 20·4, 28·6 or 36·8% contrast, and the staircase varied the contrast (in 0·05 log steps) of the component moving in the opposite direction to null any apparent motion. Results were averaged for right and left adaptation. The prediction for no direction-selective adaptation is shown by the dashed line in Fig. 2. The variable-contrast, opposite-moving

component (ordinate) was set lower in contrast than the fixed-contrast, same-moving component (abscissa), and thus direction-selective adaptation is clearly present when the test pattern is suprathreshold and the task requires the use of movement information.

Velocity matching

The following measurements tested whether the S cone signals produce a veridical velocity signal when the moving violet grating is clearly suprathreshold. The observer varied the velocity of a green luminance grating to match the apparent

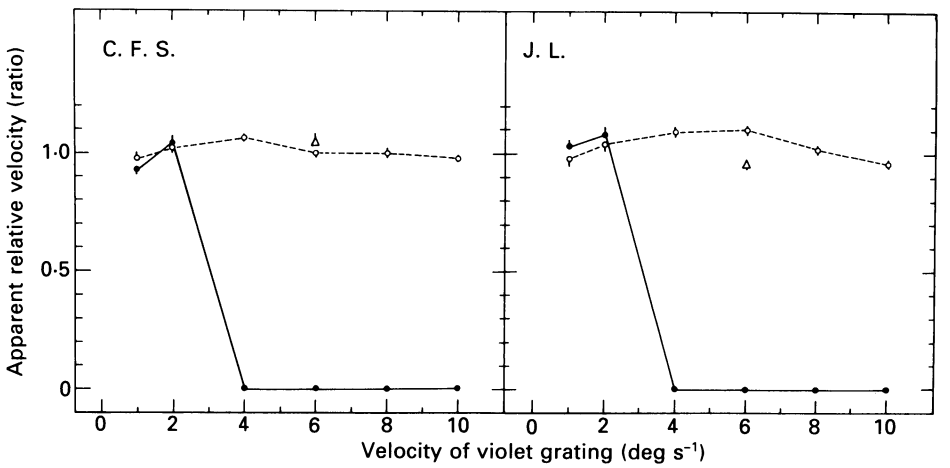

Fig. 3. Apparent velocity of rightward-moving violet grating which selectively stimulates S cones, determined by adjusting the speed of a leftward-moving green luminance grating to match the apparent speed of the violet grating. Gratings were of 1 cycle deg^{-1}, on a green adapting field. The abscissa depicts the actual velocity of the violet grating, and the ordinate depicts its apparent relative velocity – a ratio, defined as the settings of the green grating divided by the actual velocity of the violet grating. The violet grating on the green field appeared as yellowish stripes on a whitish background. ●, matches of the apparent velocity of the yellowish stripes; the stripes appeared stationary at higher velocities of 4–10 deg s^{-1}. ○, matches of the apparent velocity of the rightward streaming of the whitish background; the streaming was seen veridically (ordinate values $\cong 1{\cdot}0$). △ matches for the background streaming measured with a more intense adapting field which produces even better S cone isolation.

velocity of the violet grating. The gratings were vertical, of 1 cycle deg^{-1}. The violet grating moved rightwards in the top half of the field, while the green grating moved leftwards in the bottom half. The adapting field was green (540 nm, similar to the 538 nm spectral centroid of the green grating), and was 10·59 and 10·11 log quanta deg^{-2} s^{-1} in the top and bottom halves respectively: the top half was more intense to assure S cone isolation, while the bottom was less intense so that the green grating would be adequately visible.

The patterns were clearly visible: the green grating was of 4% luminance contrast (approximately 10× threshold) and the violet grating was of 50% S cone contrast. The top and bottom gratings abutted, and the observer stared at the central fixation point while making the matches. The two gratings were presented together in

discrete trials with the normal temporal envelope expanded twofold (Methods). For each run, the velocity of the violet grating was fixed, at the value on the abscissa of Fig. 3, and the velocity of the green grating was varied by the staircase in 0·03 log steps, with four to eight staircases devoted to each match shown in Fig. 3. The abscissa depicts the actual velocity of the violet grating, while the ordinate depicts its apparent relative velocity – a ratio, defined as the setting of the green grating divided by the actual velocity of the violet grating.

The moving violet grating on the green field appeared as saturated yellowish stripes on a whitish background field. Each of these two components might appear to move at different velocities and thus their apparent velocities were matched separately.

The motion of the whitish background (○) was seen approximately veridically, as shown by the fact that the settings are about 1·0 over the whole range. To show further that this percept of the background motion is derived from S cones, we isolated the S cones better by raising the radiance of the top adapting field to 11·22 log quanta deg^{-2} s^{-1} (129000 td). The velocity matches, performed at 6 deg s^{-1} (△), were little changed by this manipulation. The yellowish stripes (●) also appeared to move veridically at 1 and 2 deg s^{-1} – at 1 deg s^{-1} their motion appeared smooth, while at 2 deg s^{-1} it was slightly jerky. However, at 4–10 deg s^{-1} the yellowish stripes appeared stationary, and thus their velocity could not be matched even with very slow motion of the green grating.

The S cones can thus signal velocity accurately over the measured range of 1–10 deg s^{-1}, as shown by the matches for motion of the whitish background. The apparent slowing observed for the yellowish stripes might be caused by chromatic mechanisms that are unable to signal accurately rapid changes. Moreland (1982), Cavanagh, Tyler & Favreau (1984) and Livingstone & Hubel (1987) have also observed a strong apparent slowing of moving patterns defined largely by colour.

Motion mechanisms revealed by quadrature phase protocol

Directional mechanisms with S cone inputs can also be demonstrated by the quadrature phase protocol. A violet counterphase flickering mask grating of 1 cycle deg^{-1} and fixed contrast was presented in both temporal intervals of each trial. The test pattern was presented in one of the intervals. It was a similar violet counterphase grating presented in spatial–temporal quadrature phase with the mask, so as either to increase the right component of the mask and decrease the left component by the same amount, or the converse. The two different tests were achieved by shifting the temporal phase of the test by 180 deg.

Figure 4 shows the contrast threshold for detecting the test grating as a function of the mask contrast, measured at 2·95 Hz (○) and at 11·8 Hz (●). The triangles represent direction-identification thresholds, which are as low as the simple detection thresholds measured with the same conditions, indicating that the test gratings are detected by direction-selective mechanisms. The arrows on the abscissa indicate the threshold of the masks. For the lower temporal frequency, suprathreshold masks raise the test thresholds, while, at the higher temporal frequency, the masks reduce the thresholds about 2 times. The facilitation effect is similar to that observed by Stromeyer *et al.* (1984) with white gratings.

We may summarize the results thus far. The violet moving gratings on a uniform field are detected by nondirection-selective mechanisms. However, using suprathreshold patterns, we obtained evidence for direction-selective mechanisms with the paradigms of adaptation, velocity matching and quadrature phase. In addition, the direction of *rapidly* moving gratings on a uniform field can be identified when the gratings are only slightly suprathreshold.

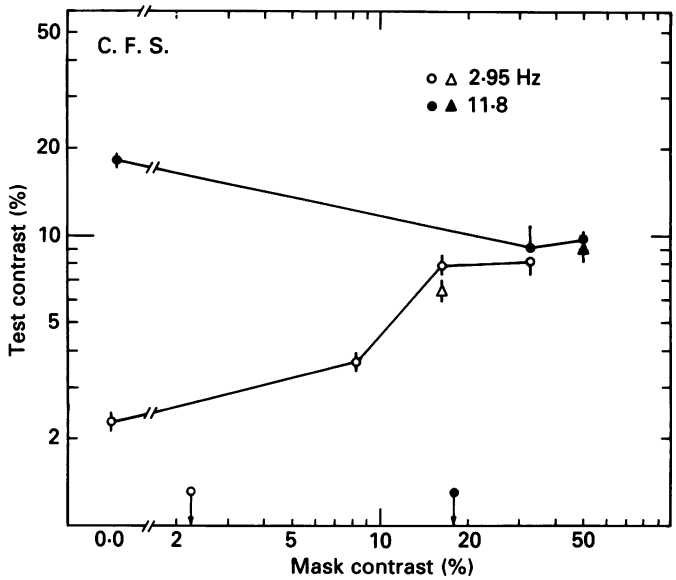

Fig. 4. Direction selectivity demonstrated with the 'quadrature' phase paradigm, with violet gratings of 1 cycle deg^{-1} on the yellow–green adapting field. Circles depict detection thresholds for a counterphase flickering test grating (ordinate) presented in spatial–temporal quadrature phase with a similar counterphase mask grating, whose contrast is depicted on abscissa (arrows indicate threshold of mask *per se*). At a temporal frequency of 2·95 Hz (○) the mask raises the test threshold, while at a frequency of 11·8 Hz (●) the mask reduces the test threshold. Thresholds for identifying the direction of motion produced by the quadrature tests (△) are as low as the detection threshold, implying that the tests are detected with direction-selective mechanisms. Contrast is specified as S cone contrast.

II. *Interaction of S cone and M and L cone signals in motion and flicker detection*

The previous measurements showed that there are motion detectors with S cone inputs. In this section the quadrature phase protocol was used to study the interaction of signals from different classes of cones within the motion detectors. On the yellow–green adapting field, an orange counterphase grating stimulates largely L cones, and the quadrature-phase violet grating stimulates largely S cones. Neither counterphase grating alone has any net motion. However, if the signals from the S and L cones are conveyed to a common direction-selective mechanism, then the combined pattern might produce a percept of right or left motion.

In the first experiment, the temporal phase of the violet grating was varied relative

to the orange grating in order to measure the relative temporal phase of the S and L cones in generating motion. Then the experiment was repeated using a uniform flickering test field of orange and violet, which demonstrated consistency between the temporal phase measurements using either a motion or luminance flicker criterion. The final experiment showed that the temporal phase measurements predict threshold summation between violet and orange gratings moving with the same velocity but with different spatial phase offsets; the results demonstrate that the *most* sensitive mechanisms for detecting rapid motion have a weak S cone input.

Relative temporal phase response of S and L cones in motion detection

For the remaining experiments the gratings were 1 cycle deg^{-1}. The mean radiances of the orange grating and yellow–green adapting field were respectively 9·26 and 10·58 log quanta deg^{-2} s^{-1}, while the radiance of violet grating was varied between experiments. The orange and violet counterphase gratings were presented together, and the observer judged whether the motion was leftward or rightward. The orange pattern was *fixed* in contrast slightly above threshold, and the staircase varied the contrast of the violet pattern to determine the direction-identification threshold of the combined pattern. Each trial contained only one observation interval.

In the first experiment several mean radiance values were used for the violet pattern, in order to vary independently the light adaptation of the S cones and measure how the phase response is thus affected. The counterphase patterns were 11·8 Hz, and the temporal phase of the violet pattern was systematically varied relative to the orange. The orange grating is represented as

$$\text{Orange}\,(x,t) = \text{Orange}_0[1 + m\cos(2\pi fx)\cos(2\pi\omega t)],$$

and the violet grating as

$$\text{Violet}\,(x,t) = \text{Violet}_0[1 + m\sin(2\pi fx)\cos(2\pi\omega t - \phi)].$$

The violet grating is shifted spatially 90 deg to the right of the orange grating, and ϕ is its temporal phase relative to the orange grating. In Figs 5–7 ϕ is plotted increasing rightwards (time increases rightwards). Positive values of ϕ thus indicate the violet grating is retarded in phase relative to the orange grating, and a rightward shift of the response curves represents a temporal advance of the S cone signal.

For a given run, the temporal phase of the violet grating had *fixed* values, ϕ and its phase-opposite, (ϕ-180 deg); the phase was switched randomly from trial to trial between these two values to produce motion in the two opposite directions. The contrast of the violet pattern was varied to determine the direction-identification threshold: the threshold for the violet pattern at ϕ and its phase-opposite are plotted at ϕ in Fig. 5.

Data points were fitted by eye with an analytical template. The strength of the differential physical motion (left *versus* right), produced by adding a violet pattern of fixed contrast, varies in proportion to $|\sin\phi|$ (providing the test is weaker than the background grating, from the last two equations of Methods). To produce a constant level of this physical motion (for a constant threshold criterion), the contrast of the violet pattern must vary as the reciprocal of this function, $|\sin\phi|^{-1}$.

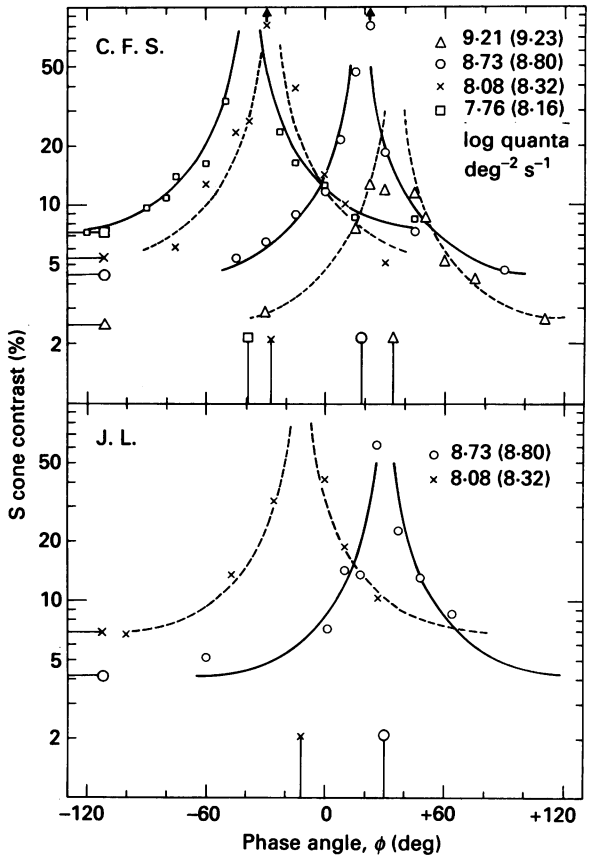

Fig. 5. Phase of S cone signal entering the motion detector, measured relative to L cone signal. Violet and orange counterphase gratings (1 cycle deg^{-1} and 11·8 Hz) on yellow–green field were presented in quadrature spatial phase, with the temporal phase ϕ of the violet grating (abscissa) set at different values relative to the orange grating. The orange grating was fixed in contrast just slightly above threshold, and the violet grating was varied in contrast (ordinate) to determine the threshold for identifying the direction of motion of the combined pattern. Measurements were made at several mean radiance values (log quanta deg^{-2} s^{-1}) of the violet pattern (inset values not in parentheses) that produce different S cone light-adaptation levels re quantal flux at 441 nm (values in parentheses). Phase data are fitted with a template, $|\sin \phi|^{-1}$; the symmetry axis is displaced laterally from $\phi = 0$ deg, indicating a physiological phase shift. The axis of each template is indicated by the vertical line at the bottom, and the horizontal asymptote is indicated by the horizontal line at the left. Phase ϕ is plotted with time increasing rightwards. Positive values indicate that the S cone signal *appears* to lead the L cone signal, and negative values indicate the S cone signal lags. (As shown later, the S cone signal is actually about one full cycle out-of-phase with the L cone signal for the template that peaks near 0 deg.) The results show that the S cone signal is relatively more delayed at low adapting levels.

The threshold data in Fig. 5 are fitted with this template function slid laterally from the symmetry axis at $\phi = 0$ deg to account for a physiological phase shift of the S cone signal relative to the L cone signal. The advantage of a template is that it uses all the data to obtain a more accurate estimate of relative phase. Lindsey, Pokorny & Smith (1986) used a similar template to assess cone phase shifts.

When the axis is centred at $\phi = 0$ deg, the left side of the template from -180 to 0 deg corresponds to leftward physical motion and the right side from 0 to $+180$ deg corresponds to rightward physical motion. The magnitude of the physical motion varies inversely with the height of the template, and thus leftward motion is strongest at $\phi = -90$ deg and rightward motion at $\phi = +90$ deg. Owing to a relative phase shift of the S cone signal (indicated by a displacement of the template axis from $\phi = 0$ deg), the *seen* motion was often the reverse direction from the physical motion. (The observer had response feedback and thus learned at the start of each run which response button to press.) On the left side of each measured template in Figs 5 and 6, the angle ϕ corresponded to leftward *seen* motion (and its opposite, ϕ-180 deg, corresponded to rightward seen motion) whereas on the right side of each template this pairing was reversed. Thus the left and right sides of each template represent left and right seen motion respectively (for angle ϕ).

At $\phi = 0$ deg the violet and orange gratings are in phase temporally, and no motion would be seen if the signals from the S and L cones were in exact temporal phase. Consider first the data represented by the circles in the top panel of Fig. 5, for a violet pattern of 8·73 log quanta deg^{-2} s^{-1}. The axis of symmetry is displaced to $+18$ deg, indicating that the S cone signal appears to lead the L cone signal by 18 deg, or 4·2 ms. (As shown later, the S cone signal is actually about one full cycle out-of-phase with the L cone signal.) The left side of the template (○) is positioned at $\phi = 0$ deg, and thus leftward motion is seen at this phase. If the phase angle is maintained at 0 deg, and a 0·65 D filter is simply placed over the violet grating, reducing the mean level to 8·08 log quanta deg^{-2} s^{-1} (×, top panel), then the seen motion reverses because the axis of symmetry shifts to -27 deg so that the right side of the template is now positioned at 0 deg. The S cone signal now appears to lag behind the L cone signal rather than to lead it. The axis can be shifted in a more extreme fashion by raising and lowering the mean radiance of the violet pattern to 9·21 and 7·76 log quanta deg^{-2} s^{-1}: the axis shifts to $+34$ deg (△, top panel) and -39 deg (□) respectively. Contrast sensitivity for this relatively high-frequency violet pattern of 11·8 Hz increases 3 times as the violet adapting level is increased over the full range (top panel), as shown by the decrease in the horizontal asymptote of the templates (left ordinate).

In the inset of Fig. 5, the values in parentheses represent the total light-adaptation level for the S cones referenced to quantal flux at 441 nm (viz. the mean of all lights in the field produce quantal catches in the S cones equivalent to a 441 nm beam of this specified flux). For C.F.S., changing the adaptive level by 1·0 log unit causes the peak to shift $\sim$ 70 deg (17 ms). The comparable values based on the limited data for the second observer J.L. (bottom panel) are 89 deg and 21 ms. The slight rightward shift in the curves for J.L., relative to C.F.S., suggests that his S cones are better stimulated by the violet light, by about 0·15 log unit, roughly corresponding to the difference of macular pigment for the two observers (Stromeyer & Lee, 1988).

The good fit of the template shows that the S cone signals feeding the motion mechanism are highly coherent (not temporally dispersed). The fact that the peaks change strongly with the radiance of the violet light implies that the violet pattern is detected with the S cones, for the light adaptation of the M and L cones is hardly affected by the violet light. It is unlikely that the M and L cones responded

significantly to the violet patterns, since the *maximal* contrast for the M and L cones was only 0·08 and 0·05% (topmost circle in Fig. 5).

From Fig. 5 we can predict that, for a violet pattern of ~ 8·4 log quanta deg^{-2} s^{-1}, the template will peak at 0 deg, indicating that the S and L cone signals are in phase

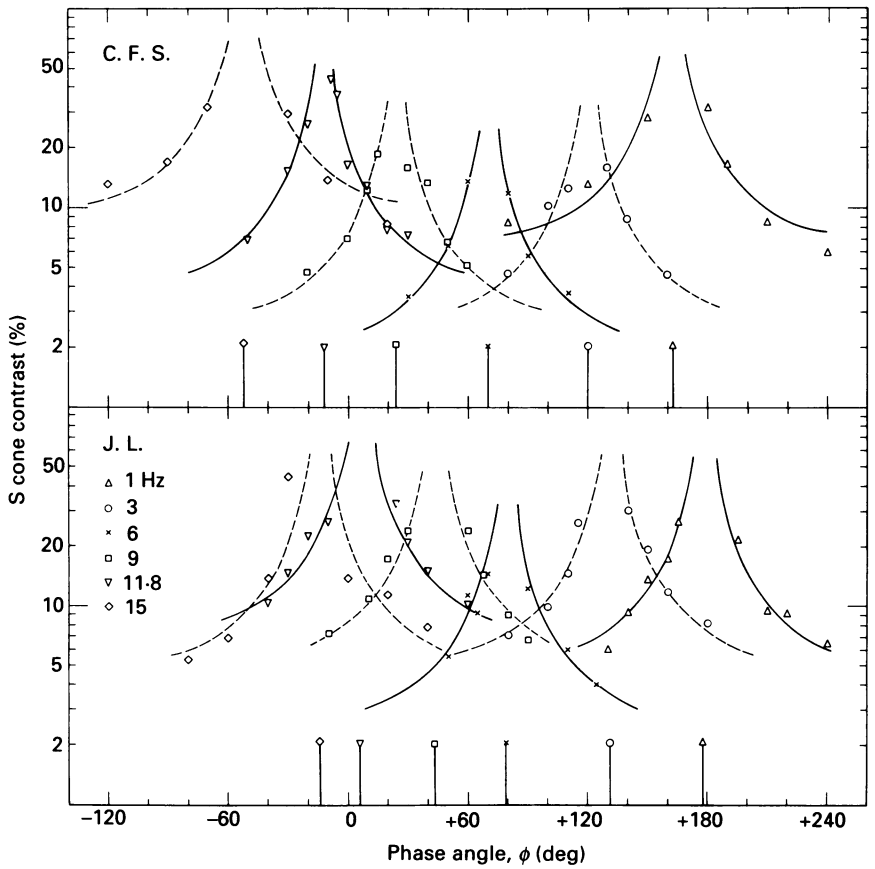

Fig. 6. Phase templates for motion detection similar to those in Fig. 5: the mean radiance of the violet pattern was 8·42 log quanta deg^{-1} s^{-1} and the temporal frequency of the violet and orange gratings were varied together from 1–15 Hz (inset). The templates shift rightwards with decreasing temporal frequency. The template position and direction of seen motion (see text) provides evidence for two components to the total phase shift: first, a phase lag of the S cone signal relative to the L cone signal, and second, the S cone signal summates negatively with the L cone signal in the motion detector and is thus effectively inverted, as shown by the apparent motion being reversed at low frequencies where the effect of the phase lag is minimal. This 'negative' summation occurs independently of temporal frequency.

relatively (i.e. phase shifts of $0 + n \times 360$ deg, n integer). Further we can predict that if the S and L cone signals are in phase in an absolute sense ($n = 0$), then the template will continue to peak at $\phi = 0$ deg as the temporal frequency is varied. This is next measured for temporal frequencies of 1–15 Hz.

Figure 6 shows how the template shifts as a function of temporal frequency. For

each curve the temporal frequency of the orange and violet gratings was identical. The mean radiance of the violet pattern was 8·42 log quanta deg^{-2} s^{-1} (the total S cone adaptive radiance, as defined above, was 8·54 log quanta deg^{-2} s^{-1}), chosen so that the curve for 11·8 Hz (△) peaks near 0 deg. The peak of the templates shifts monotonically with temporal frequency; in going from 1 Hz to 11·8 Hz this phase shift is about 1/2 cycle. This fact alone would lead us to expect that at 11·8 Hz, the seen motion would be the reverse direction from the physical motion, since the S cone signal is shifted 1/2 temporal cycle and thus temporally inverted. The seen motion, however, was not reversed. This paradox can be explained by further postulating that the S cone signal summates with a *negative sign* (an inverted sign). Thus at 11·8 Hz, the S and L cone signals appear in-phase relatively (peak at $\phi \cong 0$ deg), and the motion is not reversed for two reasons: first, there is a 1/2 cycle phase lag of the S cone signal relative to the L cone signal, and second, there is a further 1/2 cycle shift owing to the negative (inverted) sign of the S cone signal.

The data can be shown to confirm this second hypothesis as follows. We can largely eliminate the phase shift owing to the lag of the S cone signal by going to a low temporal frequency. For $\phi = +90$ deg the stimulus contains rightward physical motion, but surprisingly the results for 1 and 3 Hz show that the *left* side of the template is located at $\phi = +90$ deg; the seen motion is thus leftwards and opposite from the physical motion, which can be explained by the inverted sign of the S cone signal. (When the yellow–green adapting field was turned off, so that motion was largely signalled by the M and L cones, the seen motion was not reversed.)

Relative temporal phase of the S and L cone signals in luminance flicker discrimination

We next examined whether the phase templates for motion will predict templates for uniform flicker. The orange and violet gratings were replaced by stimuli of the same radiance as in the last experiment: 2 deg diameter coincident orange and violet uniform fields that flickered sinusoidally in the middle of the 4·2 deg yellow–green adapting field. (The smaller 2 deg fields were used to reduce stray light from the uniform violet flicker.) Each test trial had two intervals. Slightly suprathreshold orange flicker of fixed contrast was presented in both intervals (the flicker produced M cone contrast of 0·3% and L cone contrast of 1·3%). Violet flicker, of the same frequency as the orange, was added to the orange flicker at phase ϕ in one test interval and at the opposite phase ϕ-180 deg in the other interval. The amplitude of the violet flicker was the same in both intervals and was varied between trials to measure the threshold for discriminating which interval had the greater 'luminance' flicker – the criterion used by the observer and described further below. Figure 7 plots the threshold discrimination as a function of ϕ.

The flicker templates in Fig. 7 are of the same form as the motion templates (Fig. 6); however the flicker templates have all been shifted approximately 90 deg rightward along the phase axis relative to the motion templates (Fig. 6), for the following reason. Consider the curves for 11·8 Hz. For the motion task discrimination was worst for the 11·8 Hz stimuli at $\phi \cong 0$ deg because the S and L cone signals elicited by the two counterphase gratings were in phase and hence did *not* produce a motion signal. However, for the 11·8 Hz uniform flicker, discrimination is best at

$\phi \cong 0$ deg because the S and L cone signals are respectively in phase and in antiphase in the two test intervals.

The template for the flicker (unlike that for the motion) is an approximation. The observer responds to the difference of the vector sum of the flicker in the two intervals, and for a fixed

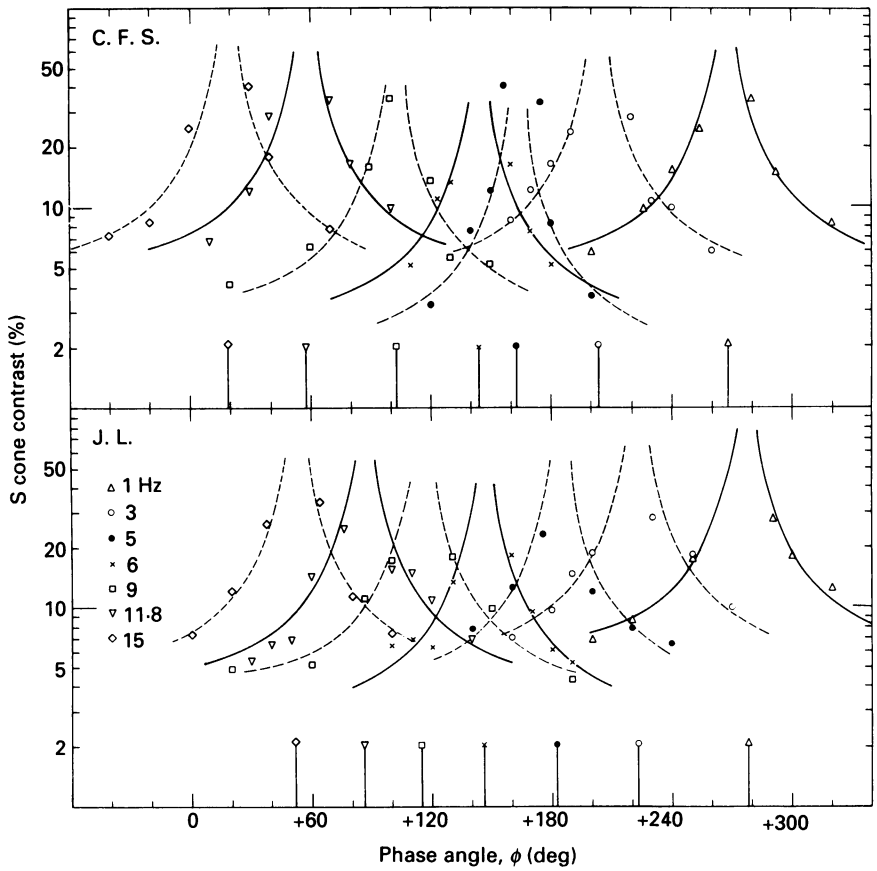

Fig. 7. Phase templates for discriminating the *luminance* flicker of a uniform, 2 deg test field of superposed violet (8·42 log quanta deg^{-2} s^{-1}) and orange lights flickering at the same frequency, in the centre of the steady yellow–green adapting field. Suprathreshold orange flicker of fixed amplitude was presented in both intervals of each test trial; violet flicker was added to the orange flicker at phase angle ϕ in one test interval and at the phase-opposite, ϕ-180 deg, in the other interval. The amplitude of the violet flicker was the same in both intervals and was varied between trials to determine the threshold for discriminating which interval had the greater 'luminance' flicker. The templates show these thresholds as a function of ϕ, measured at different temporal frequencies (inset). The templates are all shifted $\sim$ 90 deg to the right on the phase axis compared to the motion templates (Fig. 6).

threshold criterion, this difference is a constant as a function of ϕ. The function cannot be solved in closed form. However, the divergence of the template from the true function is relatively small when the violet flicker at the trough of the template (point of maximal sensitivity) is effectively small relative to the orange flicker. For stronger violet flicker, the divergence becomes appreciable only near the peak. The divergence does *not* affect the estimated symmetry axis of the template but may slightly underestimate the maximal sensitivity.

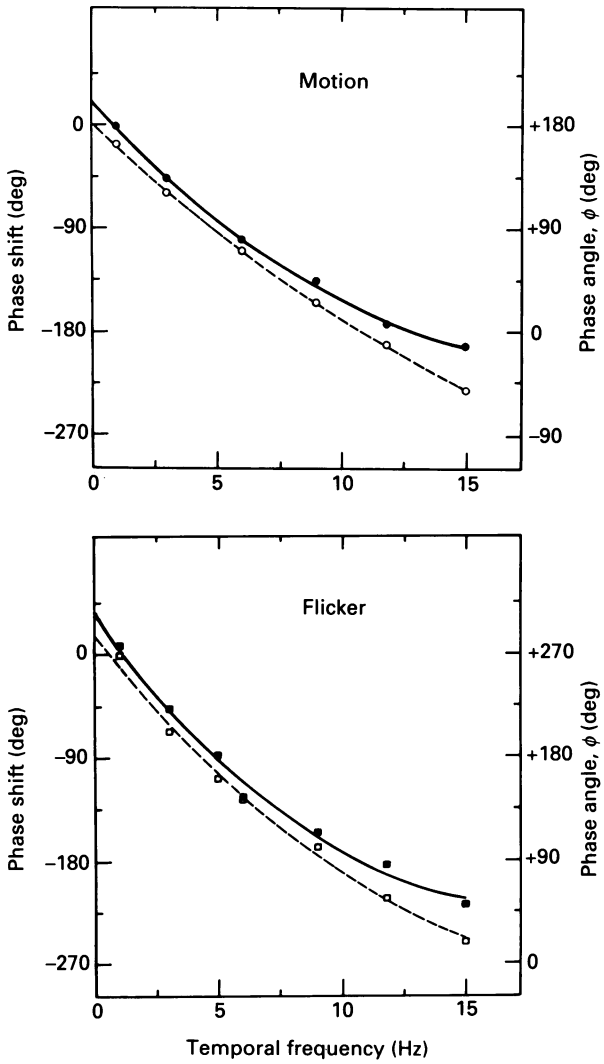

Fig. 8. Summary of phase measurements (Figs 6 and 7). The right ordinates depict the position of the peak of the phase templates as a function of temporal frequency for motion (top panel) and for luminance flicker (bottom panel). Open and filled symbols represent results for observers C. F. S. and J. L. respectively. The left ordinates represent the phase lag of the S cone signal relative to the L cone signal (not including the inversion of the sign of the S cone signal). The mean radiance of the violet stimulus was 8·42 log quanta deg^{-2} s^{-1}.

On the left side of each flicker template (Fig. 7) the test interval containing violet flicker with phase angle ϕ produced the greater luminance flicker, whereas on the right side violet flicker with the opposite phase angle, ϕ-180 deg, produced the greater luminance flicker. For 11·8 Hz, the luminance flicker was strongest when the violet and orange lights were approximately in phase (at $\phi \cong 0$ deg on the *left* side of the template). Whereas for 1 Hz, the luminance flicker was strongest when the violet and orange lights were approximately in *antiphase* (at $\phi \cong 180$ deg; again on the *left*

side of the template). Thus, the S cone signal summates with inverted sign both for the detection of motion and luminance flicker.

The observer based his flicker discrimination on the difference in the vigour of 'luminance' flicker in the two test intervals, which was an easy task at 9 Hz and above. At 6 Hz chromatic flicker became apparent and grew stronger as the frequency was reduced to 1 Hz. The observer attempted to ignore the colour in making the luminance judgements, which were both highly consistent between the two observers and well predicted from the motion data. Ikeda & Shimozono (1978) have shown that observers can make accurate heterochromatic luminance settings with square-wave flicker as low as 2 Hz, even though chromatic flicker is present.

We remeasured the phase templates at 1–5 Hz (not shown) with the same stimuli, except that the observer used any apparent chromatic difference to make his discrimination. The flicker appeared relatively more bluish and yellowish when the S and L signals were in antiphase and appeared relatively more reddish and greenish when the signals were in phase. The peaks of these chromatic templates shifted less with temporal frequency than the luminance templates, with the consequence that, at 1 Hz, the angular positions of the peaks of the luminance and chromatic templates were similar, but by 5 Hz they were highly disparate. At 1, 3 and 5 Hz respectively, the peaks of the luminance templates were at 268, 203 and 162 deg and the peaks of the chromatic templates were at 262, 260 and 238 deg for observer C.F.S. For observer J.L. the comparable peaks were at 276, 223 and 182 deg and 272, 260 and 247 deg. These results show that the S cones feed into different mechanisms which mediate the two tasks.

Figure 8 summarizes the phase results for motion and luminance flicker. The position of the peak of the templates (right ordinates) is shown as a function of temporal frequency. As described above, the flicker templates are advanced $\sim$ 90 deg on the phase axis relative to the motion templates. (The fact that the shift is somewhat less than 90 deg may be caused by the smaller violet stimulus used for the flicker task: relatively more macular pigment in the centre of the fovea would reduce S cone light adaptation and cause the S cone signals to lag more.) The left ordinates show the phase lag of the S cone signal relative to the L cone signal, determined from the templates; this lag does *not* take into consideration the negative (inverted) sign of the S cone signal. The data are fitted by smooth curves (third-order polynomial) which have no theoretical import. The phase lag does not reflect a simple delay of the S cone signal, for the curves are not straight and some curves intersect the 0 Hz axis at a positive phase angle (left ordinates), indicating a small phase lead of the S cone signal at low frequency.

Threshold summation of moving gratings

We next measured the degree of threshold summation between violet and orange gratings moving rightwards with the same velocity as a function of their relative spatial phase. The results show that when the violet and orange gratings are combined with the optimal phase, the S and L signals summate linearly for motion detection.

The mean radiances of the violet and orange gratings and the yellow–green adapting field were 8·42, 8·69 and 10·10 log quanta $deg^{-2}\,s^{-1}$. (The adapting field

intensity was reduced 3 times so that the contrast would be adequate.) The gratings moved rightwards, and the violet grating led the orange by the phase specified in Fig. 9 – the violet grating led in time and thus increasing *negative* phase represents a greater lead. To produce this lead, the violet grating was spatially advanced by different discrete values (accurate to 1 deg of spatial phase angle), set between runs by adjusting the dichroic mirror that optically combined the orange and violet patterns. Mollon & Polden (1976) observed that a moving violet bar that selectively stimulates the S cones appeared to spatially lag behind a red bar, an effect attributed to the longer latency of the short-wave π_1 mechanism. A similar temporal lag in the present experiment was compensated for by spatially advancing the violet grating relative to the orange.

Thresholds were set for seeing rightward motion of the orange grating alone, of the violet grating alone and of the two summed in different phases. The contrast ratio of the summed orange and violet gratings was fixed at the ratio of their individual thresholds, i.e. the two patterns were summed in approximately equal threshold units. The procedure was not forced-choice, for the patterns only moved rightwards (moving leftwards would have altered the phase offset of the violet grating). A single phase condition was used in each run, which contained four interleaved staircases. Each threshold estimate was based on four to twelve staircases. The observer deliberately made an error if he could not see motion, to make the staircase rise.

The degree of threshold summation, depicted on the ordinate of Fig. 9, is indicated by a summation index, representing the threshold sum of the two gratings in units of their individual thresholds. Thus

$$\text{Summation index} = \left[\frac{C_{\text{orange}}}{T_{\text{orange}}} + \frac{C_{\text{violet}}}{T_{\text{violet}}}\right],$$

where C_{orange} and C_{violet} are the contrasts of the components in the combined pattern, and T_{orange} and T_{violet} are the threshold contrasts of the patterns measured singly. A summation index of 1·0 represents complete linear summation, and values greater than about 2·0 represent partial cancellation, where the summed pattern is less visible than either component alone. The troughs of the curves in Fig. 9 represent the point of maximal sensitivity – the contrast of each component in the mixture is about half the threshold of each component measured singly. The peaks of the curves typically show cancellation.

The curves in Fig. 9 were fitted to the data by eye so as to be mirror symmetric, but otherwise of arbitrary shape. The phase angle of the peaks and troughs are quite well predicted from the templates for the counterphase gratings (Fig. 6). The latter templates specify the phase lag of the S cone signal relative to the L cone signal for motion detection (Fig. 8, top panel). These lags are indicated by arrows in Fig. 9, and they represent the amount by which the violet grating must be spatially advanced relative to the orange to bring the S and L cone signals in phase: at this point sensitivity is least, and maximal sensitivity occurs approximately 180 deg away, where the S and L signals are in antiphase. For optimal threshold summation, the violet and orange moving gratings were spatially superposed approximately in *antiphase* at 1 Hz and superposed approximately in phase at 11·8 Hz. The threshold rose maximally when the patterns were superposed in the opposite spatial phases:

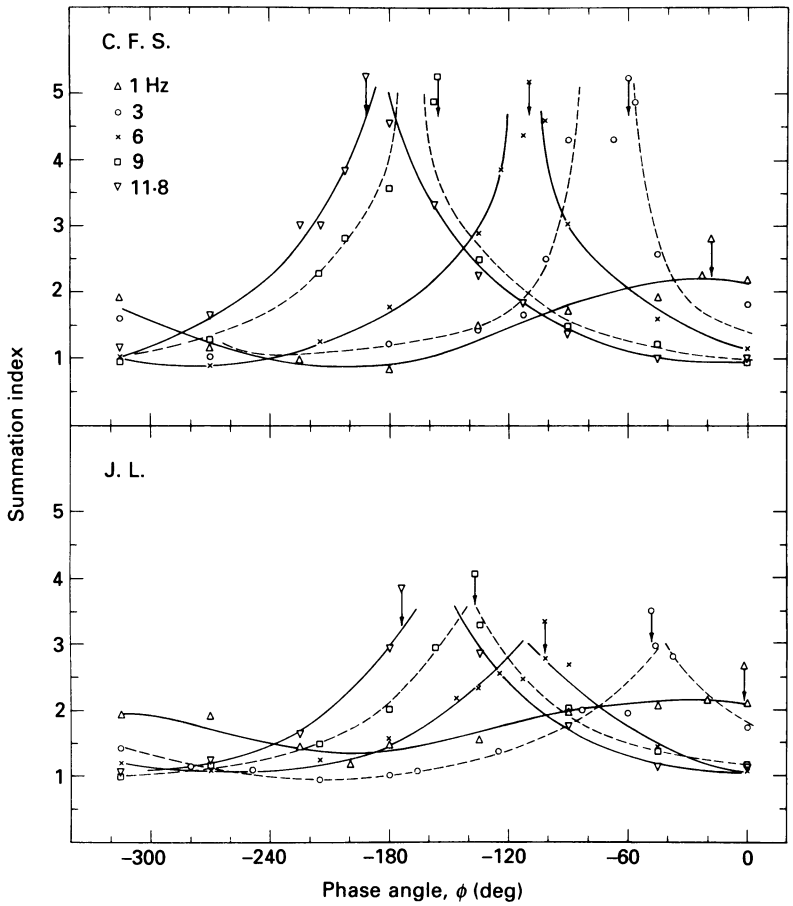

Fig. 9. Threshold summation for detecting rightward motion of a pair of violet and orange gratings (1 cycle deg^{-1}) moving rightward at the same rate (inset). Threshold summation was measured as a function of the spatial phase of the pair of gratings (abscissa), where decreasing ϕ indicates that the violet grating spatially leads the orange grating by an increasing amount. The summation index (ordinate) represents the sum of the pair of gratings at threshold, with each member grating expressed in units of its threshold measured singly: a value of 1·0 indicates complete linear summation of the violet and orange gratings for direction identification, and a value of about 2 or greater indicates partial cancellation. The arrows are the prediction of the peaks based on the results for the counterphase gratings (Fig. 6). At 1 Hz linear summation occurs when the violet and orange patterns are in spatial antiphase, while at 11·8 Hz, linear summation occurs when the patterns are in phase. The threshold summation shows that the most sensitive mechanisms for detecting rapid motion have an S cone input.

approximately in phase at 1 Hz and in antiphase at 11·8 Hz. Thus the results again support the view that the S cone signal summates with negative sign for motion detection, and at 11·8 Hz there is an ~ 180 deg phase lag of the S cone signal relative to the L cone signal.

Probability summation between *independent* S cone and L cone signals would predict flat summation curves in Fig. 9, contrary to the results. The prediction of the

degree of summation based on only probability summation was determined from frequency-of-seeing curves for identifying the direction of motion for the violet and orange gratings measured singly. Such curves were measured with the forced-choice method of constant stimuli for observer C.F.S. at 11·8 Hz. The mean radiances of the violet and orange gratings and the yellow–green adapting field were 8·42, 8·66 and 10·40 log quanta deg^{-2} s^{-1}. Each grating, was presented for 600 trials at five contrast values separated by 0·10 log unit step, and results were fitted by the Weibull function,

$$P(a) = 1-(1-1/2)\exp[-(a/\alpha)^{\beta}],$$

where $P(a)$ is probability of correct response for stimulus of amplitude a, α is the threshold at the 82% correct point, and β is the slope. The slope was particularly steep – 4·8 and 5·3 for the orange and violet gratings respectively. Probability summation (Watson *et al.* 1980) between independent responses to the orange and violet gratings would cause the threshold for each member of the paired gratings to be $\sim$ 15% less than for each grating measured singly, yielding a summation index of 1·7, and thus probability summation would contribute only a minor amount to the summation actually observed.

Threshold summation was also measured with the forced-choice direction-identification protocol. The patterns both moved left or right at 8·0 or 11·8 Hz and were spatially summed precisely in phase. For this single phase, the direction could be reversed without altering the spatial phase, and thus we were able to use the forced-choice method. The results show strong summation, suggesting the phase was approximately optimal. Three pairs of gratings were used with various adapting fields: violet and orange gratings on the yellow–green field stimulated predominantly S and L cones respectively; violet and green gratings on the orange field stimulated predominantly S and M cones respectively; and violet and orange gratings on the orange field stimulated S and M + L cones respectively. Eight or more staircases were devoted to measuring the threshold of a summed pair of gratings and the threshold of each member grating.

The first four columns of Table 3 list the various adapting fields and pairs of coloured gratings, as well as the mean radiance of each in log quanta deg^{-2} s^{-1}. The fifth column specifies the [S,M,L] cone contrasts (%) of the thresholds of the member gratings measured singly. The sixth column specifies the threshold of each member of the paired gratings in units of the threshold of the member gratings measured singly. And the right column specifies the summation index for the paired gratings, which is simply the sum of numbers in the fourth column. The fact that there is nearly complete threshold summation (summation index $\cong$ 1·0) for all pairs of coloured gratings shows that signals from all classes of cones summate in mechanisms that detect motion, and the most sensitive detectors have S cone input. The absolute threshold of the combined pattern increased considerably when a uniform field of violet light of 9·04 log quanta deg^{-2} s^{-1} was added to the display, demonstrating that the violet grating stimulates predominantly the S cones. This is shown by the increased summation index in the right column, which represents the threshold of the combined pattern with the added violet field, measured relative to the threshold of the member gratings without the added violet field.

TABLE 3. Threshold summation (see text) of pairs of moving gratings (violet, V; orange, OR; green, GR) for direction identification on yellow–green (YG) or orange (OR) adapting fields. Observers C.F.S. and J.L. in parentheses

Adapting field		Pair of gratings				Summation index	
Colour	Radiance (log quanta deg^{-2} s^{-1})	Colour	Radiance (log quanta deg^{-2} s^{-1})	[S,M,L] cone contrast (%)	Grating contrast re threshold	Without* added violet field	With added violet field
			Grating: 1 cycle deg^{-1}, 8·0 deg s^{-1}				
YG	10·58	V	7·76	[20·9, 0·006, 0·003]	0·54	0·95	1·64
		OR	8·66	[0, 0·094, 0·362]	0·41		
YG	10·58	V	8·42	[15·9, 0·010, 0·006]	0·54	1·07	1·61
		OR	8·66	[0, 0·084, 0·327]	0·53		
OR	10·72	V	8·08	[31·4, 0·047, 0·006]	0·57	1·06	1·64
		OR	8·65	[0, 0·308, 0·356]	0·49		
			Grating: 1 cycle deg^{-1}, 11·8 deg s^{-1}				
YG	10·40	V	8·42	[33·2, 0·030, 0·016]	0·52	0·96	1·73
		OR	8·66	[0, 0·108, 0·415]	0·43		
				[30·7, 0·028, 0·015]	(0·58)	(1·13)	—
				[0, 0·066, 0·253]	(0·55)		
OR	11·17	V	8·42	[37·2, 0·044, 0·006]	0·59	1·07	1·83
		GR	8·46	[1·8, 1·15, 0·233]	0·48		

* Sum of pairs of numbers in previous column.

While the S cone signals clearly summate with the M and L cone signals in motion detection, the contribution of the S cone signals is quite weak. Table 3 (fifth column) shows that for detecting the direction of motion of the 8·0 and 11·8 Hz gratings, the S cone contrast of the violet grating must be about 50 times higher than the M and L cone contrasts of the green or orange patterns. Thus in terms of the cone contrasts, the S cones only provide about 1/50 the contribution of the M and L cones. This small S cone contribution is also shown in Fig. 10, which plots C. F. S.'s thresholds for seeing motion of the violet and orange gratings that were presented singly in

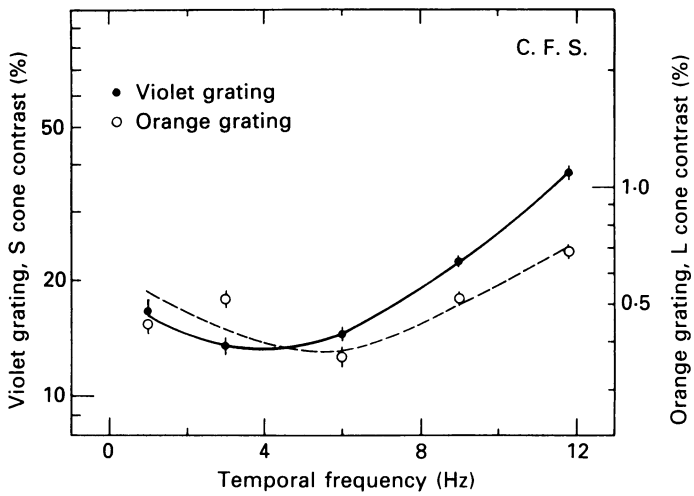

Fig. 10. Contrast thresholds for seeing rightward motion of violet and orange gratings (1 cycle deg^{-1}) presented singly and moved rightward at the rate on the absicssa. (These thresholds were obtained for the results of Fig. 9.) The left ordinate represents the S cone contrast of the violet grating, and the right ordinate represents the L cone contrast of the orange grating. The right ordinate has been shifted downwards 35 times relative to the left ordinate so the data overlap at 1-6 Hz, thus indicating that the S cone contrast sensitivity for motion at 1–6 Hz is ~ 35 times less than the L cone contrast sensitivity.

obtaining the data of Fig. 9. The right ordinate, representing the L cone contrast of the orange grating, has been shifted downwards 35 times relative to the left ordinate, representing the S cone contrast of the violet grating, so that the data overlap at 1–6 Hz. Thus at 1–6 Hz, the S cone contrast sensitivity for motion is about 35 times less than the L cone contrast sensitivity. For observer J. L. the S cones were about 50 times less sensitive. The curve for the violet grating shows that the S cone signal entering the motion detector declines rather gradually with temporal frequency, and should be contrasted with the very steep decline Wisowaty & Boynton (1980) obtained for detecting S cone flicker. At low temporal frequency, the flicker is likely detected by sensitive chromatic mechanisms.

III. *Transient tritanopia and motion detection*

The previous results showed that in detecting motion, signals from the S cones and the M and L cones are summated. The final experiment measures whether the S cone

signal initially proceeds through a spectrally antagonistic site before this summation. The S cone signal might be diminished by polarizing the antagonistic site by dimming an intense yellow adapting field that itself causes few quantal catches in the S cones – an effect known as transient tritanopia (Mollon & Polden, 1977). The present experiment demonstrates transient tritanopia for S cone signals that enter motion detectors.

The observer adapted to an intense yellow (580 nm, 10·88 log quanta deg^{-2} s^{-1}) adapting field, which was either presented continuously or dimmed by 1·24 log units for 800 ms every 6·0 s. During the time period corresponding to the dimmed phase,

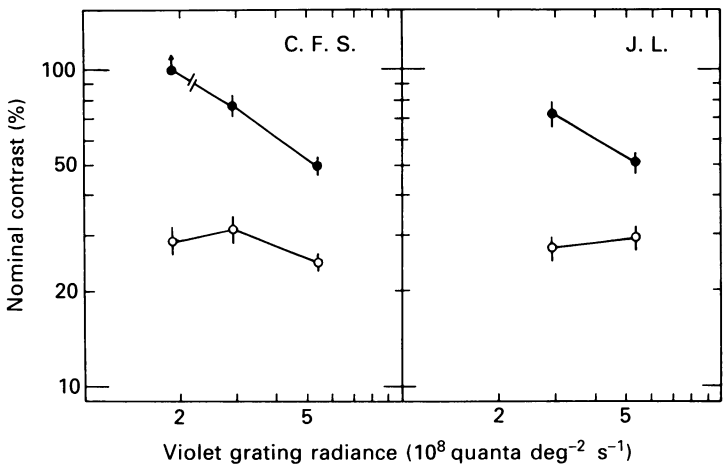

Fig. 11. Transient tritanopia for identifying direction of motion. Nominal contrast thresholds (contrast of violet CRT *per se*) are shown for identifying direction of a moving violet grating (1 cycle deg^{-1}, 8 deg s^{-1}) as a function of its mean radiance. Thresholds either were measured on a steady yellow adapting field of 580 nm and 10·88 log quanta deg^{-2} s^{-1} (○) or were measured just after this field was dimmed by 1·24 log units, every 6·0 s (●). For all measurements, the mean radiance of the violet grating was increased from zero to the value on the abscissa during the 800 ms time period corresponding to the dimmed phase, and the grating modulation was turned on for the first 470 ms of this 800 ms period. Dimming the yellow adapting field reduces sensitivity to the motion of the violet grating, suggesting that the S cone signal proceeds through a spectrally antagonistic site before summating in the motion detector.

the violet test field was exposed by opening a shutter for 800 ms, and the grating modulation was turned on for the first 470 ms. (The cosine temporal ramps were reduced to 19 ms). The test pattern consisted of a 1 cycle deg^{-1} grating that moved leftwards or rightwards at 8 deg s^{-1}, and the observer identified its direction in the forced-choice protocol.

An important feature of the procedure is that the mean radiance of the test pattern increased from zero to a positive value during the 800 ms that the shutter was open. If the mean radiance of the relatively intense violet patterns had instead been kept constant, dimming the yellow field may have resulted in little transient tritanopia (Augenstein & Pugh, 1977). Thus, it was expected that simultaneously dimming the

yellow field light and augmenting the radiance of the violet test light would strongly polarize the antagonistic site and hence might produce clear transient tritanopia.

Figure 11 shows the nominal contrast threshold for identifying the direction of motion of the violet gratings as a function of the mean radiance of the violet gratings. Open circles depict thresholds measured with the steady yellow field, and filled circles depict thresholds measured during the transient dimming of the yellow field. Transient tritanopia is clearly shown by the strong threshold rise when the yellow field is dimmed. The effect is weaker for the higher radiance patterns, for the patterns (●) might be detected by the M cones that recover rapidly during the dimming phase, as shown next. The experiment was repeated with a moving green grating (8·40 log quanta deg^{-2} s^{-1}) substituted for the violet one: dimming the yellow field caused the direction-identification threshold to *fall* 9·1 and 9·3 times for C. F. S. and J. L. respectively.

Transient tritanopia was also clearly present for higher velocity 11·8 deg s^{-1} violet (8·73 log quanta deg^{-2} s^{-1}) patterns: dimming caused the direction-identification threshold to rise 70 and 100% for C. F. S. and J. L. These experiments thus suggest that the S cone signals first proceed through a spectrally antagonistic site before they summate with other cone signals in motion detectors.

DISCUSSION

Dichotomy of mechanisms with S cone inputs

We first consider features of the results which suggest that S cone signals contribute to non-directional mechanisms, possibly of a chromatic nature, and to mechanisms that analyse motion or luminance flicker. S cones also contribute to the analysis of orientation (Stromeyer, Kronauer, Madsen & Cohen, 1980) and stereopsis (Grinberg & Williams, 1985).

In the first experiments, violet gratings of 1 cycle deg^{-1} were presented on a yellowish field. Gratings of 3–12 Hz were detected at threshold by non-directional mechanisms, as shown by the low threshold ratio of counterphase and moving gratings, and by the fact that the moving gratings had to be raised above detection threshold to identify the direction of motion. Watson *et al.* (1980) obtained similar results for slow moving achromatic patterns, detected by non-directional mechanisms. We were also unable to obtain clear evidence for directional mechanisms using threshold-level test patterns in a motion adaptation protocol. The violet gratings at the detection threshold typically had a chromatic appearance of yellowish stripes on a whitish background with little motion or flicker. When the moving gratings were clearly suprathreshold, as in the velocity matching experiment, two percepts were produced: that of streaming motion in the whitish background, which was seen veridically, and that of essentially stationary yellowish stripes at physical velocities of 4–10 deg s^{-1}.

Observations with the violet gratings provide evidence for less sensitive directional mechanisms: first, at 11·8 Hz the direction of motion was identified only very slightly above detection threshold. Second, direction-selective adaptation was strong when the test pattern was suprathreshold and the task required the use of motion information. Third, velocity matching showed that suprathreshold patterns produce

veridical motion – streaming in the whitish background. And fourth, a counterphase test presented in quadrature phase with a similar mask, had equivalent detection and direction-identification thresholds, implying the test was detected by directional mechanisms.

Results with pairs of coloured stimuli provide further evidence for separate chromatic and luminance or directional mechanisms receiving S cone inputs, for the phase templates measured with violet and orange stimuli differed strongly when discrimination was based on a chromatic criterion *versus* a luminance or motion criterion.

Measurements by Stockman *et al.* (1987) with selective temporal masks also suggest that the S cone signal has access to two mechanisms: a low-pass temporal mechanism that may provide chromatic information, and a bandpass temporal mechanism that processes luminance information.

S cone input to luminance mechanisms

Signals from the S cones summate linearly with the M and L cones for motion detection, as implied by the results for identifying the motion of pairs of coloured gratings. The S cone signal summated with a negative sign, and was thus inverted, as demonstrated by three findings. (1) The peak of the phase templates for violet and orange counterphase gratings was extrapolated to $\sim$ 180 deg at 0 Hz. Thus at low temporal frequencies the direction of seen motion was opposite that of the physical motion. (2) The inversion was also demonstrated by threshold summation of orange and violet gratings moving with the same velocity. At low temporal frequencies, the gratings produced a strong motion signal when summed approximately in spatial antiphase, and motion was harder to see when the gratings were summed in phase. (3) The inversion of the S cone signal was also observed with low-frequency uniform flicker: luminance flicker was stronger with the orange and violet lights in temporal antiphase rather than in phase.

Stockman *et al.* (1987) have also argued that the S cone signal is inverted within the luminance channel. They determined the relative phase angle that produced the best apparent null for violet and red flicker on an intense orange adapting field; the results when extrapolated from 5–25 Hz to 0 Hz showed an inversion of the S cone signal.

The following considerations suggest that S cone signals have access to luminance pathways. Heterochromatic flicker photometry, which is used to equate the luminance of different spectral lights, is thought to equate the action of the lights within a luminance channel that linearly summates M and L cone signals. This hypothesis is supported by psychophysical studies showing spectral additivity for heterochromatic flicker photometry (Ikeda, 1983) and for the detection of rapid flicker (Stromeyer, Cole & Kronauer, 1987). The methods of 'minimum perceived motion' (Moreland, 1982) and the 'nulling of apparent motion' (Cavanagh *et al.* 1987) also equate the luminance of different spectral lights, and the latter method is spectrally additive within a few per cent (Kaiser, Vimal, Cowan & Hibino, 1987). These studies thus suggest that the most sensitive mechanisms used for detecting rapid flicker or motion respond to the linear sum of M and L cone signals.

The detection of rapid flicker and motion in the present experiments is likely to

involve the same sensitive luminance mechanisms. Consider the results for the threshold summation of pairs of moving gratings (Table 3). The spectrally long-wave component, moving at 8 or 11·8 Hz, produced a percept of formless left or right rapid motion at the threshold for detecting direction, and little if any colour modulation was seen. The luminance contrast sensitivity was very high for the long-wave component, 300–500 at 8 Hz (Table 3). (Luminance contrast sensitivity can be defined approximately as the reciprocal of one-half the sum of threshold-level M and L cone contrasts; Stromeyer *et al.* 1987). Now when we add a violet grating to the long-wave grating, we obtain linear summation of the two patterns for motion detection. This implies that the S cone signal is linearly summing, albeit with negative sign, within the same highly sensitive mechanism that detects the motion of the long-wave grating.

Eisner & MacLeod (1980) concluded that the S cones did not contribute to the luminance channel, as tested by flicker photometry. However, Stockman & MacLeod (1986) observed visible beats between high-frequency (< 40 Hz) subthreshold S cone flicker and suprathreshold L cone flicker, which they attributed to the luminance channel (Stockman *et al.* 1987). Drum (1983) has also measured a contribution of S cones to achromatic sensitivity in an increment threshold task.

Cavanagh *et al.* (1987), however, were unable to identify an S cone contribution to the luminance channel, as assessed by nulling of apparent motion. The present results show that the S cone contribution to motion detection may be only $\sim 1/50$ that of the M and L cones, with the contributions expressed as cone contrasts. This weak S cone contribution is probably too small to be positively identified with the method of Cavanagh *et al.* (1987). They presented simultaneously a counterphase luminance grating and a 'quadrature' counterphase chromatic grating and had the observer adjust the luminance contrast of the latter to null apparent motion. The settings were highly similar whether the S cones were strongly bleached (rendered largely ineffective) or not. However, if the S cones contributed only 1/50 the amount of the M and L cones to detection of the motion, then the settings would be expected to change $\sim 0{\cdot}009$ log units (2%) upon bleaching the S cones. They measured such tiny effects, but concluded that the effects might reflect a change in the action spectra of the M and L cones owing to the bleaching, rather than a small contribution by S cones.

The present study shows that the S cones signals contribute to the detection of motion in addition to subserving colour vision. Studies of the discharges of single neurones in the macaque's lateral geniculate nucleus (Derrington & Lennie, 1984; Derrington, Krauskopf & Lennie, 1984) have revealed a dichotomy of mechanisms with S cone inputs. The parvocellular type II cells that receive S cone inputs in opposition to M and L cone inputs are thought to be important for colour vision and have very low contrast sensitivity to moving achromatic gratings. On the other hand, the magnocellular cells, many of which have S cone inputs, have high contrast sensitivity (Kaplan & Shapley, 1982) to moving achromatic gratings, and Derrington *et al.* (1984) suggest that these latter neurones may contribute to a specialized system for detecting motion. Our results on the threshold summation for moving gratings indicate that the detection mechanisms have *very high* luminance contrast sensitivity to the long-wave component grating, while also having low contrast sensitivity to the

violet grating signalled by S cones. The results on transient tritanopia suggest that signals from the S cones initially proceed through a spectrally antagonistic site before summation in the motion mechanism.

Temporal properties of the S cone pathways

We measured the relative lag of the S and L cone signals for identifying the direction of motion produced by the violet and orange gratings. For a moderate S cone light-adapting level (8·54 log quanta deg^{-2} s^{-1} at 441 nm, Fig. 6), the S cone signal lagged behind the L by $\sim 1/2$ cycle at 11·8 Hz (42 ms). Varying the adapting level from 8·16 to 9·23 log quanta deg^{-2} s^{-1} caused the S cone lag to vary by ~ 70 deg (from 51 to 34 ms; observer, C.F.S.). Stockman *et al.* (1987 and personal communication) obtained similar results for the interaction of S and L cone signals assessed with uniform flicker. Interpolated means for three observers with 10 Hz flicker revealed an S cone lag that varied from 46 to 29 ms over the same range of S cone adaptation. The response of the S cone pathway thus becomes faster with increased light adaptation. This was also demonstrated by Brindley, DuCroz & Rushton (1966) and Wisowaty & Boynton (1980) who showed that the temporal resolution of the S cone pathway, as measured by the critical fusion frequency, increased in proportion to the log intensity of the adapting field (Ferry–Porter law).

These results might at first seem contradictory to the observations of Krauskopf & Mollon (1971) and Friedman *et al.* (1984) that the short-wave π_1 and π_3 mechanisms of Stiles have a long and approximately constant temporal integration period (critical duration) of about 200 ms, which is invariant with the state of light adaptation either of the S cones or the spectrally antagonistic site in this pathway (Friedman *et al* 1984). The critical duration is probably determined by the most sensitive mechanism, which may be a chromatic one. Long critical durations have been measured in studies that enforce detection by a chromatic mechanism (Regan & Tyler, 1971). The S cones might also have access to other luminance or motion channels with shorter temporal integration; however, these channels may simply not express themselves in the critical duration of π_1 and π_3.

The decreased S cone lag that we observe with increased light adaptation may result from a change in the S cones *per se*, for electrical recordings demonstrate the response of cones becomes faster with increased light adaptation (Baylor & Hodgkin, 1974; Baron & Boynton, 1975). The temporal properties of the S cones may not differ from other classes of cones, as shown by intracellular recordings in the macaque (Baylor, 1986) and by recordings of the isolated PIII component of the electroretinogram (ERG) in the ground squirrel (Crognale & Jacobs, 1988). Crognale & Jacobs (1988), however, showed that the b-wave of the ERG was significantly slower for the S cones then for the M cones. Thus the S cone lag may be largely postreceptoral.

This research was supported by NIH EY-01808 and AFOSR 86-0338. We are grateful to R. Land for help in early stages of this work and to P. Cavanagh, R. T. Eskew Jr, R. E. Kronauer, A. Reeves and A. Stockman for their advice.

REFERENCES

AUGENSTEIN, E. J. & PUGH JR, E. N.(1977). The dynamics of the Π_1 colour mechanism: further evidence for two sites of adaptation. *Journal of Physiology* **272**, 247–281.

BARON, W. S. & BOYNTON, R. M. (1975). Response of primate cones to sinusoidally flickering homochromatic stimuli. *Journal of Physiology* **246**, 311–331.

BAYLOR, D. A. (1986). Photoreceptor signals and vision. *Investigative Ophthalmology and Visual Science* **28**, 34–49.

BAYLOR, D. A. & HODGKIN, A. L. (1974). Changes in time scale and sensitivity in turtle photoreceptors. *Journal of Physiology* **242**, 729–758.

BRINDLEY, G. S., DUCROZ, J. J. & RUSHTON, W. A. H. (1966). The flicker fusion frequency of the blue-sensitive mechanism of colour vision. *Journal of Physiology* **183**, 497–500.

CAVANAGH, P., MACLEOD, D. I. A. & ANSTIS, S. M. (1987). Equiluminance: spatial and temporal factors and the contribution of blue-sensitive cones. *Journal of the Optical Society of America* A **4**, 1428–1438.

CAVANAGH, P., TYLER, C. W. & FAVREAU, O. E. (1984). Perceived velocity of moving chromatic gratings. *Journal of the Optical Society of America* A **1**, 893–899.

CROGNALE, M. & JACOBS, G. H. (1988). Temporal properties of the short-wavelength cone mechanism: comparison of receptor and postreceptor signals in the ground squirrel. *Vision Research* **28**, 1077–1082.

DERRINGTON, A. M., KRAUSKOPF, J. & LENNIE, P. (1984). Chromatic mechanisms in lateral geniculate nucleus of macaque. *Journal of Physiology* **357**, 241–265.

DERRINGTON, A. M. & LENNIE, P. (1984). Spatial and temporal contrast sensitivities of neurones in lateral geniculate nucleus of macaque. *Journal of Physiology* **357**, 219–240.

DRUM, B. (1983). Short-wavelength cones contribute to achromatic sensitivity. *Vision Research* **23**, 1433–1439.

EISNER, A. & MACLEOD, D. I. A. (1980). Blue-sensitive cones do not contribute to luminance. *Journal of the Optical Society of America* **70**, 121–123.

FRIEDMAN, L. J., YIM, M. H. & PUGH JR, E. N. (1984). Temporal integration of the π_1/π_3 pathway in normal and dichromatic vision. *Vision Research* **24**, 743–750.

GRINBERG, D. L. & WILLIAMS, D. R. (1985). Stereopsis with chromatic signals from the blue-sensitive mechanism. *Vision Research* **25**, 531–537.

HOLLINS, M. & ALPERN, M. (1973). Dark adaptation and pigment regeneration in human cones. *Journal of General Physiology* **62**, 430–447.

IKEDA, M. (1983). Linearity law reexamined for flicker photometry by the summation-index method. *Journal of the Optical Society of America* **73**, 1055–1061.

IKEDA, M. & SHIMOZONO, H. (1978). Luminous efficiency functions determined by successive brightness matching. *Journal of the Optical Society of America* **68**, 1767–1771.

KAISER, P. K., VIMAL, R. L. P., COWAN, W. & HIBINO, H. (1987). Luminance measured by nulling of apparent motion: an additivity experiment. *Investigative Ophthalmology and Visual Science*, suppl., **28**, 93.

KAPLAN, E. & SHAPLEY, R. M. (1982). X and Y cells in the lateral geniculate nucleus of macaque monkeys. *Journal of Physiology* **330**, 125–143.

KRAUSKOPF, J. & MOLLON, J. D. (1971). The independence of the temporal integration properties of individual chromatic mechanisms in the human eye. *Journal of Physiology* **219**, 611–623.

LEVINSON, E. & SEKULER, R. (1975). The independence of channels in human vision selective for direction of movement. *Journal of Physiology* **250**, 347–366.

LINDSEY, D. T., POKORNY, J. & SMITH, V. C. (1986). Phase-dependent sensitivity of heterochromatic flicker. *Journal of the Optical Society of America* A **3**, 921–927.

LIVINGSTONE, M. S. & HUBEL, D. H. (1987). Psychophysical evidence for separate channels for the perception of form, color, movement, and depth. *Journal of Neuroscience* **7**, 3416–3468.

MOLLON, J. D. & KRAUSKOPF, J. (1973). Reaction time as a measure of the temporal response properties of individual colour mechanisms. *Vision Research* **13**, 27–40.

MOLLON, J. D. & POLDEN, P. G. (1976). Some properties of the blue cone mechanism of the eye. *Journal of Physiology* **254**, 1-2*P*.

MOLLON, J. D. & POLDEN, P. G. (1977). An anomaly in the response of the eye to light of short wavelengths. *Philosophical Transactions of the Royal Society* B **278**, 207–240.

MORELAND, J. D. (1982). Spectral sensitivity by motion photometry. In *Documenta Ophthalmologica Proceedings Series*, vol. 33, ed. VERRIEST, G., pp. 61–66. The Hague: Dr W. Junk Publishers

PUGH JR, E. N. & MOLLON, J. D. (1979). A theory of the π_1 and π_3 color mechanisms of Stiles. *Vision Research* **19**, 293–312.

REGAN, D. & TYLER, C. W. (1971). Temporal summation and its limit for wavelength changes: an analog of Bloch's Law for color vision. *Journal of the Optical Society of America* **61**, 1414–1421.

SEKULER, R. & GANZ, L. (1963). Aftereffect of seen motion with a stabilized retinal image. *Science* **139**, 419–420.

SMITH, V. C. & POKORNY, J. (1975). Spectral sensitivity of the foveal cone photopigments between 400 and 500 nm. *Vision Research* **15**, 161–171.

STILES, W. S. (1953). Further studies of visual mechanisms by the two-colour threshold method. In *Coloquio Sobre Problemas Opticos de la Vision*, pp. 65–103, Madrid: Union Internationale de Physique Pure et Appliquée.

STOCKMAN, A. & MACLEOD, D. I. A. (1986). Visible beats from invisible flickering lights: evidence that blue-sensitive cones respond to rapid flicker. *Investigative Ophthalmology and Visual Science*, suppl., **27**, 71.

STOCKMAN, A., MACLEOD, D. I. A. & DEPRIEST, D. D. (1987). An inverted S-cone input to the luminance channel: evidence for two processes in S-cone flicker detection. *Investigative Ophthalmology and Visual Science*, suppl., **28**, 92.

STROMEYER III, C. F., COLE, G. R. & KRONAUER, R. E. (1987). Chromatic suppression of cone inputs to the luminance flicker mechanism. *Vision Research* **27**, 1113–1137.

STROMEYER III, C. F., KRONAUER, R. E., MADSEN, J. C. & COHEN, M. A. (1980). Spatial adaptation of short-wavelength pathways in humans. *Science* **207**, 555–557.

STROMEYER III, C. F., KRONAUER, R. E., MADSEN, J. C. & KLEIN, S. A. (1984). Opponent-movement mechanisms in human vision. *Journal of the Optical Society of America* A **1**, 876–884.

STROMEYER III, C. F. & LEE, J. (1988). Adaptational effects of short wave cone signals on red–green chromatic detection. *Vision Research* **28**, 931–940.

WATSON, A. B., THOMPSON, P. G., MURPHY, B. J. & NACHMIAS, J. (1980). Summation and discrimination of gratings moving in opposite directions. *Vision Research* **20**, 341–347.

WETHERILL, G. B. (1963). Sequential estimation of quantal response curves. *Journal of the Royal Statistical Society* B **25**, 1–48.

WISOWATY, J. J. & BOYNTON, R. M. (1980). Temporal modulation sensitivity of the blue mechanism: measurements made without chromatic adaptation. *Vision Research* **20**, 895–909.